Neuronal Nitric Oxide Synthase: Substrate and Solvent Kinetic Isotope Effects on the Steady-State Kinetic Parameters for the Reduction of 2,6-Dichloroindophenol and Cytochrome c^{3+} †

Kirsten R. Wolthers‡ and Michael I. Schimerlik*,‡,§

Department of Biochemistry and Biophysics and Environmental Health Sciences Center, Oregon State University, Corvallis, Oregon 97331

Received May 8, 2001; Revised Manuscript Received October 19, 2001

ABSTRACT: The neuronal nitric oxide synthase (nNOS) basal and calmodulin- (CaM-) stimulated reduction of 2,6-dichloroindophenol (DCIP) and cytochrome c^{3+} follow ping-pong mechanisms [Wolthers and Schimerlik (2001) *Biochemistry 40*, 4722−4737]. Primary deuterium [NADPH(D)] and solvent deuterium isotope effects on the kinetic parameters were studied to determine rate-limiting step(s) in the kinetic mechanisms for the two substrates. nNOS was found to abstract the *pro-R* (A-side) hydrogen from NADPH. Values for ^{D}V and $^{D}(V/K)_{NADPH}$ were similar for the basal (1.3−1.7) and CaM-stimulated (1.5−2.1) reduction of DCIP, while ^{D}V (2.1−2.8) was higher than $^{D}(V/K)_{NADPH}$ (1.1−1.5) for cytochrome c^{3+} reduction with and without CaM. This suggests that the rate of the reductive half-reaction (NADPH oxidation) rather than that of the oxidative half-reaction (reduction of DCIP or cytochrome c^{3+}) limits the overall reaction rate. A value for $^{D}(V/K)_{NADPH}$ close to 1 indicates the intrinsic isotope effect on hydride transfer is suppressed by a slower step in the reductive half-reaction. The oxidative half-reaction is insensitive to NADPD isotope effects as both $^{D}(V/K)_{DCIP}$ and $^{D}(V/K)_{cytc}$ equal 1 within experimental error. Large solvent kinetic isotope effects (SKIE) observed for $(V/K)_{cytc}$ for basal (∼8) and CaM-stimulated (∼31) reduction of cytochrome c^{3+} suggest that proton uptake from the solvent limits the rate of the oxidative half-reaction. This step does not severely limit the overall reaction rate as ^{D_2O}V equaled 2 and $^{D_2O}(V/K)_{NADPH}$ was between 0.9 and 1.3 for basal and CaM-stimulated cytochrome c^{3+} reduction.

Mammalian nitric oxide synthase (NOS)[1] consumes 1.5 NADPH and 2 O_2 in the two-step conversion of L-arginine to NO and L-citrulline (*1*). All three known isoforms of NOS, neuronal (nNOS), endothelial (eNOS), and inducible (iNOS), function as homodimers (*1*). Each polypeptide subunit is divided into an oxygenase domain, which contains a P450-type heme and the binding sites for (6*R*)-5,6,7,8-tetrahydrobiopterin (H_4B) and L-arginine (*2*), and a reductase domain, which contains FAD, FMN, and the binding site for NADPH (*3*). During catalysis the flavins transfer NADPH-derived electrons to the oxygenase domain to enable heme-based oxygen activation and subsequent oxidation of L-arginine (*4*). The binding of Ca^{2+}-activated calmodulin (Ca^{2+}-CaM) to the CaM-binding motif located between the two domains facilitates electron transfer between the flavins and the heme (*5*). A rise in intracellular Ca^{2+} concentration triggers the binding of CaM to eNOS and nNOS (*6*); however, CaM remains tightly bound to iNOS at basal levels of Ca^{2+} (*7*).

The NOS reductase domain is structurally and functionally similar to cytochrome P450 reductase (CPR). Amino acid alignment of the last 641 residues on nNOS revealed 36% sequence identity and 58% sequence homology with CPR (*3*). nNOS and CPR are both composed of an NADPH−FAD module, homologous to ferridoxin−$NADP^+$ reductase (FNR), and an FMN module that is homologous to bacterial flavodoxin (*3*, *8*, *9*). The mode of electron transfer in NOS and CPR is proposed to proceed from NADPH to FAD to FMN and then finally to the heme (*10*, *11*). The flavins on NOS and CPR are thought to cycle between the one- and three-electron reduced states during catalysis (*12*, *13*). Finally, both NOS and CPR are able to reduce nonphysiological electron acceptors such as ferricyanide (FeCN), 2,6-dichloroindophenol (DCIP), and cytochrome c^{3+} (*14*, *15*). The binding of Ca^{2+}-CaM to nNOS and eNOS alleviates partial inhibition of electron transfer to these substrates (*16*), as DCIP and FeCN reduction increases 2−3-fold and cytochrome c^{3+} reduction increases 10−20-fold (*17*). The CaM-stimulated reduction of these nonphysiological substrates is not linked to electron transfer to the heme, to production of superoxide (*13*), or to a change in the redox potentials of the flavins (*11*). Ca^{2+}-CaM does increase pre-steady-state flavin reduction (*16*, *18*) and induces confor-

† This work was supported by Grant ES00210 from the National Institute of Environmental Health Sciences.

* To whom correspondence should be addressed at the Department of Biochemistry and Biophysics, Agricultural and Life Sciences Building 2011, Oregon State University, Corvallis, OR 97331. Telephone: (541) 737-2029. Fax: (541) 737-0481. E-mail: schimerm@onid.orst.edu.

‡ Department of Biochemistry and Biophysics, Oregon State University.

§ Environmental and Health Sciences Center, Oregon State University.

[1] Abbreviations: NOS, nitric oxide synthase; NO, nitric oxide; nNOS, neuronal NOS; eNOS, endothelial NOS; iNOS, inducible NOS; H_4B, (6*R*)-5,6,7,8-tetrahydrobiopterin; Ca^{2+}-CaM, Ca^{2+}-activated calmodulin; CPR, NADPH−cytochrome P450 oxidoreductase; FNR, ferridoxin−$NADP^+$ reductase; FeCN, ferricyanide; DCIP, 2,6-dichloroindophenol; cyt *c*, cytochrome c^{3+}; 2′AMP, 2′-adenosine monophosphate; G6PDH, glucose-6-phosphate dehydrogenase; DHFR, dihydrofolate reductase; NADPD, (4*R*)-[^{2}H]NADPH; ^{D}V, deuterium isotope effect on V_{max}; $^{D}(V/K)$, deuterium isotope effect on V_{max}/K_m; ^{D_2O}V, solvent isotope effect on V_{max}; $^{D_2O}(V/K)$, solvent isotope effect on V_{max}/K_m.

10.1021/bi0109461 CCC: $22.00
Published on Web 12/08/2001

mational changes in the diflavin domain (*19*). The structural rearrangement may remove the autoinhibitory effects of a 45−50 amino acid insert located in the middle of the FMN-binding domain of eNOS and nNOS (*20*). This insert, which is not found in other structurally related flavoproteins or iNOS, promotes the dissociation of CaM at low intracellular Ca^{2+} concentrations and inhibits electron transfer in the absence of Ca^{2+} (*21*, *22*). Additionally, Ca^{2+}-CaM may interact with the 20 amino acid C-terminal tail to promote interflavin electron transfer. The C-terminal tail, unique to the NOS isoforms, inhibits electron transfer to nonphysiological electron acceptors in the absence of Ca^{2+}-CaM (*18*, *23*).

In lieu of a three-dimensional crystal structure of NOS depicting the specific structural role of CaM, an understanding of how the activated cofactor imparts control of electron transfer relies on the above-mentioned and future biochemical and mutagenesis studies as well as comparative analysis with structurally related enzymes. Steady-state kinetic data for the basal and CaM-stimulated reduction of cytochrome c^{3+} catalyzed by nNOS were shown to be consistent with a nonclassical two-site ping-pong mechanism, which is similar to the mechanism previously described for the CPR cytochrome c^{3+} reductase activity (*24*). Ternary complexes are permissible for this kinetic mechanism as the substrate active sites and the catalytic activities do not overlap. In contrast, the kinetic mechanism for basal and CaM-stimulated reduction of DCIP is limited to the formation of binary complexes as kinetic data for this substrate are consistent with a ping-pong bi-bi mechanism. In this paper, primary deuterium isotope effects using NADPD and solvent isotope effects were employed to identify possible rate-limiting step(s) in these kinetic mechanisms. nNOS was found to abstract the *pro-R* hydrogen from NADPH. Primary deuterium [NADPH-(D)] isotope effects on *V* and *V/K* for basal and CaM-stimulated DCIP and cytochrome c^{3+} reduction suggest that, of the two half-reactions, the reductive half-reaction involving NADPH oxidation limits the overall reaction rate. However, a small value for $^{D}(V/K)$ indicates that hydride transfer to FAD is not the slow step within the reductive half-reaction. Large solvent kinetic isotope effects (SKIE) observed for $(V/K)_{cytc}$ suggest that proton uptake is the rate-limiting step in the oxidative half-reaction. However, proton uptake does not limit the overall reaction rate since small SKIE on *V* and $(V/K)_{NADPH}$ were observed.

EXPERIMENTAL PROCEDURES

Materials. The cDNA for rat neuronal NOS was kindly provided by T. M. Dawson (Johns Hopkins University, Baltimore, MD; *25*), and the pCWori(+) expression vector was a gift from F. W. Dalhquist (University of Oregon, Eugene, OR; *26*). Tetrahydrobiopterin (H_4B) was purchased from Cayman Chemical Co. (Ann Arbor, MI), 2′,5′-ADP−Sepharose was from Amersham Pharmacia Biotech (Piscataway, NJ), and the TSK-GEL TOYOPEARL DEAE-650M (65 μm resin) was bought from Supelco (Bellefont, PA). Hepes was purchased from Research Organics (Cleveland, OH). Ammonium acetate, from EM Scientific (Gibbstown, NJ), was prepared from reagent grade crystals, and the pH was adjusted to 7.5 with NH_4OH. NADPH, $NADP^+$, DCIP, cytochrome c^{3+}, dihydrofolate, yeast glucose-6-phosphate dehydrogenase (G6PDH; 260 UI/mg), *Aspergillus niger* glycerol dehydrogenase (0.227 unit/mg), and yeast hexokinase (270 UI/mg) were also purchased from Sigma (St. Louis, MO). D-[1-^{3}H(N)]Glucose (specific activity of 11.3 Ci/mmol) was obtained from New England Nuclear (Boston, MA). D_2O (D, 99.9%) and deuterated glycerol (1,1,2,3,3-D_5, 99%) were from Cambridge Isotope Laboratories (Andover, MA). T4 bacteriophage dihydrofolate reductase (DHFR) was a gift from Dr. Christopher Mathew's laboratory (Oregon State University), and calmodulin and calmodulin−Sepharose were donated by Drs. Sonia Anderson and Dean Malencik (Oregon State University).

Preparation of [4(S)-^{3}H]NADPH. The procedure for the synthesis of [4(*R*)-^{3}H]NADPH and [4(*S*)-^{3}H]NADPH was adapted from Moran et al. (*27*). A 0.1 mL sample containing 1 μCi (8.7 nmol) of [^{3}H]glucose dissolved in 95% ethanol was dried with a gentle stream of argon. [1-^{3}H]Glucose was then dissolved in 100 μL of 50 mM Tris-HCl (pH 7.8) containing 1 μmol of $MgCl_2$ and 0.1 μmol of ATP and phosphorylated to give [1-^{3}H]glucose 6-phosphate with the addition of 0.5 unit of hexokinase (*28*). After incubation at room temperature for 10 min, the reaction volume was brought to 0.2 mL with H_2O. Ten nanomoles of $NADP^+$ and 0.5 unit of G6PDH were added to generate [4(*S*)-^{3}H]-NADPH. The reaction was incubated at room temperature for 30 min, then brought to a volume of 1 mL with H_2O, and applied to an 8.4 mL (1.2 cm^2 × 7 cm) TSK-GEL TOYOPEARL DEAE-650M (65 μm resin) column equilibrated with 10 mM ammonium acetate at 4 °C. An 80 mL linear gradient from 10 mM to 0.75 M ammonium acetate was applied to the column at a flow rate of 0.5 mL/min, and 0.8 mL fractions were collected. The amount of tritium in a 10 μL sample was determined by liquid scintillation counting. Fractions with an A_{260}/A_{340} absorbance ratio ≤2.4 and a high specific activity (∼8.5 Ci/mmol) were pooled.

Preparation of [4(R)-^{3}H]NADPH. To synthesize [4(*R*)-^{3}H]NADPH, the purified [4(*S*)-^{3}H]NADPH was converted to [4-^{3}H]$NADP^+$ by DHFR, which stereospecifically removes the unlabeled 4 *pro-R* hydrogen (*29*). The reaction mixture containing the pooled fraction of [4(*S*)-^{3}H]NADPH, 42 mM β-mercaptoethanol, 0.133 mM dihydrofolate, and 0.5 unit of T4 bacteriophage DHFR was incubated at room temperature for 10 min, then diluted to 60 mL with H_2O, and applied to an 8.4 mL (1.2 cm^2 × 7 cm) TSK-GEL TOYOPEARL DEAE-650M (65 μm resin) column equilibrated with 10 mM ammonium acetate at 4 °C. An 80 mL linear gradient from 10 mM to 0.75 M ammonium acetate was applied to the column at a flow rate of 1 mL/min. Fractions were collected (1 mL), and fractions with a high specific activity having A_{260} absorbance without an A_{340} absorbance were pooled. B-face reduction of the nicotinamide ring was accomplished using G6PDH by adding the following to approximately 6 mL of [4-^{3}H]$NADP^+$: 19.8 mM glucose 6-phosphate, 60 mM $MgCl_2$, and 0.5 unit of G6PDH. The reaction was incubated at room temperature for 10 min before dilution with 50 mL of H_2O and purification on TSK-GEL TOYOPEARL DEAE-650 as described above. Fractions with a high specific activity (2.53 Ci/mmol) were combined.

Preparation of [4(R)-^{2}H]NADPH. [4(*R*)-^{2}H]NADPH was synthesized with the addition of 0.1 unit of glycerol dehyrdrogenase from *A. niger* to a 1 mL mixture containing 2 mM $NADP^+$ and 10 mM deuterated (1,1,2,3,3-D_5) glycerol

in 50 mM glycine/NaOH (pH 9.0). The reaction was incubated at room temperature for 45 min, and the production of NADPH was followed by an increase in absorbance at 340 nm. The enzyme was then heat inactivated by immersing the reaction for 2 min in a water bath at 41 °C. The reaction was applied to a 20 mL (1.2 cm^2 × 14 cm) TSK-GEL TOYOPEARL DEAE-650M column equilibrated with 10 mM ammonium acetate, pH 7.5. A 100 mL linear gradient from 0.01 to 1 M ammonium acetate was applied to the column at a flow rate of 0.75 mL/min, and 1 mL fractions were collected. Fractions with an A_{260}/A_{340} absorbance ratio ≤2.4 were pooled and used in the substrate kinetic isotope studies. The concentration of NADP(H/D) was determined spectrophotometrically using $\epsilon_{340} = 6.22\ mM^{-1}\ cm^{-1}$ (*30*).

nNOS Expression and Purification. Recombinant rat nNOS was purified from *Escherichia coli* strain BL21(DE3) after overexpression of the cDNA with the pCWori(+) vector. The enzyme was purified according to the protocol published by Gerber and Ortiz de Montellano with slight modification (*31*). nNOS was more than 85% pure as judged by SDS−polyacrylamide gel electrophoresis with a specific activity of 150 nmol of NO $min^{-1}\ mg^{-1}$ at 25 °C. The rate of NO production was measured by the hemoglobin−NO capture assay following the procedures of Stuehr et al. (*32*). Protein concentration was determined with the Lowry assay using BSA as a standard (*33*).

Determining the Stereospecificity of nNOS-Catalyzed NADPH Hydride Transfer. The procedure for determining the stereospecificity of hydride transfer was adapted from Vanoni and Matthews (*34*). The hemoglobin−NO capture assay was used to determine which hydrogen was transferred under conditions of NO synthesis. A 1 mL reaction mixture containing 0.1−0.3 μM [4(*R*)-^{3}H]NADPH or 0.7 μM [4(*S*)-^{3}H]NADPH and 4 μM oxygenated hemoglobin, 5 μM FAD, 100 μM L-arginine, 10 μM $CaCl_2$, 100 nM CaM, and 8 μM H_4B was incubated with 1 μg of nNOS at 25 °C for 30 min. Duplicate reaction mixtures, lacking nNOS, were also incubated under the hemoglobin−NO capture assay conditions to determine the extent of nonenzymatic tritium release into the solvent. The stereospecificity of hydride transfer under uncoupled NADPH oxidation conditions was determined by addition of 10 μM $CaCl_2$ and 100 nM CaM to either 0.1−0.3 μM [4(*R*)-^{3}H]NADPH or 0.7 μM [4(*S*)-^{3}H]-NADPH. Finally, to examine if Ca^{2+}-CaM influences the stereospecificity of hydride transfer, 0.1−0.3 μM [4(*R*)-^{3}H]-NADPH] or 0.7 μM [4(*S*)-^{3}H]NADPH was incubated along with 50 μM DCIP and 1 μg of nNOS at 25 °C for 30 min. At the completion of the reaction the radioactivity released from the solvent was separated from radioactive NADPH and/or $NADP^+$ by condensation of the solvent on a cold finger. Solvent fractions from reactions with and without nNOS were collected from the cold finger (∼1 mL), and solute fractions from the enzymatic and the nonenzymatic reactions were collected and redissolved in 1 mL of H_2O. The amount of radioactivity in each sample was then analyzed by liquid scintillation counting.

Determination of $^D(V/K)$ and ^DV Associated with the Oxidation of [4(R)-^{2}H]NADPH. The [4(*R*)-^{2}H]NADPH eluted from the column at 0.5 M ammonium acetate. Fractions containing [4(*R*)-^{2}H]NADPH were pooled, and the concentration was determined at 340 nm using $\epsilon_{340} = 6.22\ mM^{-1}\ cm^{-1}$. A stock of the same concentration was then made of [4(*R*)-^{1}H]NADPH from Sigma in 0.5 M ammonium acetate. Primary kinetic substrate isotope effects were determined by direct comparison of the initial rates for reduction of cytochrome c^{3+} ($\Delta\epsilon = 21.1\ mM^{-1}\ cm^{-1}$) at 550 nm or DCIP ($\Delta\epsilon = 21\ mM^{-1}\ cm^{-1}$) at 600 nm (*35*) with [4(*R*)-^{2}H]-NADPH or [4(*R*)-^{1}H]NADPH. Reactions were performed in 3.5 mL at 25 °C using a 5 cm path-length cuvette. Reaction mixtures contained 50 mM Hepes (pH 7.5), variable concentrations of substrates [4(*R*)-^{2}H]NADPH or [4(*R*)-^{1}H]-NADPH, cytochrome c^{3+} or DCIP, and, where appropriate, 10 μM $CaCl_2$ and 100 nM CaM. Reactions were initiated with the addition of 0.5−2 μg of nNOS. nNOS-catalyzed reductions of DCIP and cytochrome c^{3+} follow ping-pong mechanisms; thus, *V* and *V/K* for the substrates, NADPH, DCIP, and cytochrome c^{3+} were obtained by directly fitting initial velocities at varying [4(*R*)-^{2}H]NADPH or [4(*R*)-^{1}H]-NADPH concentrations with varying DCIP or cytochrome c^{3+} concentrations to eq 1 with Origin v 4.0 software (MicroCal Software Inc., North Hampton, MA). In eq 1, v_i

$$v_i = \frac{VAB}{K_A B + K_B A + AB} \tag{1}$$

is the initial velocity, *V* is the maximal velocity, *A* is the concentration of [4(*R*)-^{2}H]NADPH or [4(*R*)-^{1}H]NADPH, and *B* is the concentration of DCIP or cytochrome c^{3+}, and K_A and K_B are their corresponding Michaelis constants. *V/K* values were then computed by dividing the fitted values of *V* and either K_A or K_B and propagating the error. Reciprocal initial velocities were plotted against the reciprocal substrate concentrations, and in all cases, the plots were linear. ^DV, equal to V_H/V_D, was calculated by dividing V_H for experiments containing [4(*R*)-^{1}H]NADPH by V_D, determined with [4(*R*)-^{2}H]NADPH as a substrate. $^D(V/K)$ is the ratio $(V/K)_H/(V/K)_D$, where $(V/K)_H$ and $(V/K)_D$ were determined with [4(*R*)-^{1}H]NADPH or [4(*R*)-^{2}H]NADPH as the substrate. A control experiment showed that [4(*R*)-^{1}H]NADPH prepared in the same manner as [4(*R*)-^{2}H]NADPH exhibited the same kinetic parameters as [4(*R*)-^{1}H]NADPH purchased from Sigma.

Solvent Kinetic Isotope Effects. A 50 mM Hepes solution in D_2O was prepared by two lyophilizations of a 50 mM Hepes solution in H_2O, each time redissolving the dry residue in D_2O. pD values were determined by adding 0.4 to the pH meter reading (pD = pH + 0.4; *36*). For reactions performed in D_2O, nNOS and CaM were diluted in D_2O, and stock solutions of NADPH, cytochrome c^{3+}, DCIP, and $CaCl_2$ were prepared by dissolving their lyophilized powders into D_2O. The SKIE on $(V/K)_{DCIP}$ was determined by measuring the initial rate of DCIP reduction at varying DCIP concentrations with a fixed, subsaturating concentration of NADPH (0.25 μM). Since both basal and CaM-stimulated reductions of DCIP follow a ping-pong mechanism, the concentration of NADPH will not influence the values of $(V/K)_{DCIP}$ (*24*); however, the value of *V* could not be determined since the NADPH concentration was not saturating. The data were fit to the Michaelis−Menten equation (eq 2) by nonlinear least-squares analysis with Origin v 4.0 software:

$$v_i = \frac{VA}{K_m + A} \tag{2}$$

Table 1: Stereospecificity of the Oxidation of NADP(H/T) Catalyzed by nNOS

substrate	concn (μM)	dpm released into solvent		dpm retained in residue	
		+enzyme	−enzyme	+enzyme	−enzyme
[4(*R*)-^{3}H]NADPH					
HbO_2[a]	0.1	217223 (74)[d]	22218 (10)	57336 (26)	211839 (90)
	0.3	664264 (84)	74046 (13)	109134 (16)	570954 (87)
	0.3	753876 (89)	92192 (14)	88408 (11)	640829 (86)
uncoupled[b]	0.3	641646 (81)		123281 (19)	
DCIP[c]	0.3	814592 (87)		110381 (13)	
[4(*S*)-^{3}H]NADPH					
HbO_2	0.7	99201 (3)	154542 (5)	2933589 (97)	3345873 (96)
	0.7	78604 (3)	140567 (4)	2993746 (97)	3133324 (97)
	0.7	228073 (9)	55513 (2)	2465362 (91)	3138312 (98)
uncoupled	0.7	100706 (3)		3213992 (97)	
DCIP	0.7	487964 (17)		2869820 (83)	

[a] NADPH oxidation was performed under conditions of the HbO_2 assay described in Experimental Procedures. [b] NADPH oxidation was performed in the absence of L-arginine. [c] DCIP was used as the terminal electron acceptor for NADPH oxidation. [d] Percent of counts in the reaction mixture is given in parentheses.

where v_i is the initial velocity, V is the maximal velocity, A is the variable substrate concentration, and K_m is the Michaelis constant for A. The SKIE on V and $(V/K)_{cytc}$ was determined by comparing the initial rate of cytochrome c^{3+} reduction at increasing concentrations of cytochrome c^{3+} and saturating concentrations of NADPH (10 μM) in 50 mM Hepes (pH/D 7.5) prepared in H_2O or D_2O. A nonlinear least-squares fit of the data to eq 2 gave values for V and K_m for cytochrome c^{3+}. $(V/K)_{cytc}$ was then calculated as described above. Since concentrations of cytochrome $c^{3+} > 5K_m$ inhibits the reduction of the electron acceptor, the SKIE on $(V/K)_{NADPH}$ was determined by measuring cytochrome c^{3+} reduction with varying NADPH concentrations at a fixed subsaturating concentration of cytochrome c^{3+} (0.4 μM). The data were fit to the Michaelis−Menten equation (eq 2) by nonlinear least-squares analysis.

RESULTS

Stereospecificity of nNOS-Catalyzed NADPH Oxidation. The stereospecificity of NADPH oxidation was determined under conditions for NO synthesis, uncoupled NADPH oxidation, and NADPH oxidation with DCIP as an electron acceptor. Table 1 shows that, under each of these conditions, the *pro-R* hydrogen is abstracted. Approximately 85% of the tritium was released into the solvent in the presence of nNOS with [4(*R*)-^{3}H]NADPH as the substrate. The majority of the tritium remained with the residue in the absence of nNOS. The percentage of tritium released into the solvent was the same in the absence and presence of the enzyme with [4(*S*)-^{3}H]NADPH as the substrate. On the basis of these results, nNOS catalyzes the stereospecific removal of the *pro-R* hydrogen at the 4-position of NADPH, and the subsequent exchange of this hydrogen with the solvent occurs, possibly on the enzyme-bound flavin.

Substrate Isotope Effects with [4(R)-^{2}H]NADPH. [4(*R*)-^{1}H]NADPH was prepared in the same manner as [4(*R*)-^{2}H]-NADPH to ensure that the synthesized NADPH had the same properties as NADPH purchased from Sigma. The synthesized [4(*R*)-^{1}H]NADPH exhibited the same V and K_m for NADPH compared to [4(*R*)-^{1}H]NADPH purchased from Sigma (data not shown). The primary deuterium isotope effects on ^DV and $^D(V/K)$ listed in Table 2 are ratios of V_H/V_D and $(V/K)_H/(V/K)_D$, respectively, which were obtained by fitting initial velocities at varying concentrations of [4(*R*)-^{1}H]NADPH or [4(*R*)-^{2}H]NADPH with varying concentrations of DCIP or cytochrome c^{3+} to eq 1, as described in Experimental Procedures. The values for $^D(V)$ in the presence and absence of Ca^{2+}-CaM with DCIP as the terminal electron acceptor were 1.56 ± 0.10 and 1.91± 0.33, respectively. $^D(V/K)_{NADPH}$ for basal activity was 1.42 ± 0.13 while CaM-stimulated activity produced a value of 1.60 ± 0.17. $^D(V/K)_{DCIP}$ with and without Ca^{2+}-CaM was 1.02 ± 0.10 and 1.01 ± 0.10, respectively, indicating that the oxidative half-reaction is isotopically insensitive to hydride transfer.

Table 2: Measurement of ^DV and $^D(V/K)$ for nNOS-Catalyzed NADPH Oxidation[a]

substrate	Ca^{2+}-CaM	^DV	$^D(V/K)_{NADPH}$	$^D(V/K)_{acc}$
DCIP	−	1.56 ± 0.10	1.42 ± 0.13	1.01 ± 0.10
DCIP	+	1.91 ± 0.33	1.60 ± 0.17	1.02 ± 0.10
cyt c^{3+}	−	2.72 ± 0.07	1.19 ± 0.10	0.98 ± 0.07
cyt c^{3+}	+	2.24 ± 0.16	1.31 ± 0.16	0.97 ± 0.04

[a] Reaction conditions are described under Experimental Procedures. Values are from a global fit of eq 1 to three experiments ± standard errors.

$^D(V)$ for basal reduction of cytochrome c^{3+} was 2.72 ± 0.07. In the presence of Ca^{2+}-CaM, $^D(V)$ equaled 2.24 ± 0.16. The value for $^D(V/K)_{NADPH}$ was 1.31 ± 0.16 and 1.19 ± 0.10 in the presence and absence of Ca^{2+}-CaM, respectively. $(V/K)_{cytc}$ did not exhibit an NADPH(D) primary isotope effect in either the presence (0.97 ± 0.04) or absence (0.98 ± 0.07) of Ca^{2+}-CaM, since the values were 1 within experimental error. The lack of an observed NADPD isotope effect on the oxidative half-reaction with DCIP and cytochrome c^{3+} is consistent with the reactions following ping-pong mechanisms and further suggests that the label exchanges with the solvent prior to reduction of these two substrates (*34*).

Solvent Kinetic Isotope Effects on Kinetic Parameters. Solvent kinetic isotope studies involve comparing the values of V and V/K for various substrates (NADPH, DCIP, and cytochrome c^{3+}) in buffer prepared in H_2O or D_2O. The deuterium in D_2O exchanges with all of the hydrogenic sites on nNOS and the substrates; therefore, D_2O has the potential to affect V and V/K by altering substrate binding and/or affecting the stability or conformation of the enzyme (*37*). To determine if the latter contributed to the observed SKIE, nNOS and the substrates (NADPH, DCIP, and cytochrome

Table 3: Kinetic Solvent Isotope Effect on Kinetic Parameters for NADPH Oxidation[a]

substrate	Ca^{2+}-CaM	^{D}V	$^{D}(V/K)$
NADPH	−		0.87 ± 0.08[b]
NADPH	+		1.17 ± 0.07[b]
DCIP	−	nd[c]	0.72 ± 0.07
DCIP	+	nd	3.97 ± 0.32
cyt c^{3+}	−	1.99 ± 0.06	8.38 ± 0.69
cyt c^{3+}	+	2.07 ± 0.09	31.00 ± 2.99

[a] Reaction conditions are described under Experimental Procedures. Values are generated from a global fit to eq 2 of three experiments ± standard errors. [b] Determined with cytochrome c^{3+} as the second substrate. [c] Not determined.

c^{3+}) were equilibrated in D_2O, and the catalytic rates of DCIP and cytochrome c^{3+} reduction were compared to nNOS and the three substrates diluted in H_2O under identical conditions. No differences in catalytic rates were observed; therefore, the observed solvent isotope effects are not attributed to an irreversible change in the structure of the enzyme itself.

The solvent isotope effects on the kinetic parameters for the reduction of DCIP and cytochrome c^{3+} are summarized in Table 3. An inverse solvent isotope effect, 0.72 ± 0.07, was observed for $(V/K)_{DCIP}$ for the basal reduction of this electron acceptor. However, in the presence of Ca^{2+}-CaM the value for $^{D_2O}(V/K)_{DCIP}$ was equal to 3.97 ± 0.32. A large SKIE was observed for the basal reduction of cytochrome c^{3+} with a value for $^{D_2O}(V/K)_{cytc}$ of 8.38 ± 0.69. This value increased approximately 4-fold in the presence of Ca^{2+}-CaM to 31.00 ± 2.99. The values for ^{D_2O}V for the basal and CaM-stimulated reduction of cytochrome c^{3+} were equal within error, 1.99 ± 0.06 (basal) and 2.07 ± 0.09 (Ca^{2+}-CaM). The large SKIE associated with $(V/K)_{cytc}$ indicates that proton uptake from the solvent is the rate-determining step in the half-reaction involving the reduction of this substrate (*37*). Since the value for ^{D_2O}V is ~2 for the basal and CaM-stimulated reduction of cytochrome c^{3+}, proton uptake does not completely limit the rate of the overall reaction. Values for $^{D_2O}(V/K)_{NADPH}$ of 0.87 ± 0.08 and 1.17 ± 0.07 for the basal and CaM-stimulated reduction of cytochrome c^{3+}, respectively, indicate that proton transfer is not a rate-limiting step in the reductive half-reaction.

DISCUSSION

Stereospecificity of nNOS-Catalyzed NADPH Oxidation. The separate NADPH/FAD and FMN binding modules of nNOS and other related dual flavoproteins such as CPR (*9*), sulfite reductase (*38*), and methionine synthase reductase (*39*) are homologous to FNR and flavodoxin, respectively. FNR is the prototypic member of the transhydrogenase family of proteins which also includes NADH−nitrate reductase and NADH−cytochrome b_5 reductase (*8*, *40*). Enzymes in this family catalyze the transfer of electrons between nicotinamide nucleotides (obligate two-electron or hydride donors/acceptors) and obligate one-electron donors (*40*). The stereospecificity of hydride transfer appears to be a conserved feature for this enzyme family as members including FNR (*41*), CPR (*42*), NADPH−cytochrome b_5 reductase (*43*), and NADH−nitrate reductase (*44*) were shown to abstract the *pro-R* hydrogen. A second class of flavin-containing enzymes, the carbon−sulfur transhydrogenase family, are stereospecific for the *pro-S* hydrogen (*40*). Enzymes of this family, including glutathione reductase (*28*), thioredoxin reductase (*45*), and lipoamide dehydrogenase (*46*), catalyze two-electron transfers between nicotinamide nucleotides and disulfide−dithiol pairs.

As shown in Table 1, the *pro-R* hydrogen is abstracted during nNOS-catalyzed NADPH oxidation. Therefore, nNOS obeys the relationship between the class of transhydrogenases and stereospecificity of hydride transfer.

Substrate Isotope Effects. Establishing that the *pro-R* hydrogen is stereospecifically removed permitted investigation of the primary isotope effects of [4(*R*)-^{2}H]NADPH on basal and CaM-stimulated DCIP and cytochrome c^{3+} reduction. The ^{D}V and $^{D}(V/K)$ values (Table 2) will be used to describe rate-limiting step(s) in the ping-pong kinetic mechanisms previously reported for the nNOS-catalyzed reduction of these two substrates. The two half-reactions consist of reduction of the enzyme-bound flavin by NADPH and release of the oxidized nucleotide (reductive half) followed by the binding of the oxidant, DCIP or cytochrome c^{3+}, and reoxidation of the reduced flavin (oxidative half).

Steady-state initial velocity and inhibition studies have shown that the ping-pong kinetic mechanisms for DCIP and cytochrome c^{3+} reduction are different. Basal and CaM-stimulated DCIP reduction follows a classical single-site ping-pong bi-bi mechanism (Figure 3 in ref *24*) whereas the initial velocity and inhibition patterns for the basal and CaM-stimulated reduction of cytochrome c^{3+} are consistent with a two-site ping-pong mechanism (*24*).[2] The salient feature of the latter mechanism is the ability of NADPH and cytochrome c^{3+} to act at catalytically independent sites on nNOS, permitting ternary complexes to form. The derivation of these two kinetic mechanisms produced identical expressions for $(V/K)_{NADPH}$:

$$\left(\frac{V/E_t}{K_A}\right) = \frac{k_3}{K_{iA}(1 + 1/K)} \qquad (3)$$

where V is the maximal velocity, E_t is the concentration of nNOS, K_A is the Michaelis constant for NADPH, K_{iA} is the NADPH dissociation constant, K is the equilibrium constant for the conversion of E_1 to E_1', and k_3 is the rate constant for hydride transfer. In both kinetic mechanisms, only the rate constant representing hydride transfer, k_3, is sensitive to isotopic substitution of NADPH; thus, the expression for a substrate isotope effect on $(V/K)_{NADPH}$ is

$$^{D}(V/K)_{NADPH} = {}^{D}k_3 \qquad (4)$$

where $^{D}k_3$ equals k_{3H}/k_{3D} with k_{3H} defining the rate of NADPH hydride transfer and k_{3D} the rate of NADPD deuteride transfer. As shown in eq 4, $^{D}(V/K)_{NADPH}$ equals $^{D}k_3$, the intrinsic isotope effect on hydride transfer. Typically, the value of the intrinsic isotope effect ranges between 5 and 8, which corresponds to the differences between the zero-point vibrational energies of C−H and C−D bonds in the ground and transition states, but values are observed outside this range due to the nature of the transition state or tunneling (*47*). Thus, the value of $^{D}(V/K)_{NADPH}$ should fall within this

[2] These mechanisms are identical to those shown in Figures 1 and 2 of this paper, with the exception that the charge-transfer complex was omitted.

range. However, as shown in Table 2, the value for $^{D}(V/K)_{NADPH}$ was much lower for the basal or CaM-stimulated reduction of DCIP or cytochrome c^{3+}. This suggests that $^{D}(V/K)_{NADPH}$ is composed of more rate-limiting isotopically insensitive step(s) that suppress the value of $^{D}k_3$ (*48*). The other microscopic rate constants defining $(V/K)_{NADPH}$ may include binding and release of NADPH or conformational changes occurring after NADPH binding (see below).

Previous steady-state dead-end inhibition experiments suggest that NADPH binds in rapid equilibrium (*24*). The NADPH analogue, 2′AMP, was shown to be a competitive dead-end inhibitor versus varying concentrations of NADPH at fixed concentrations of DCIP or cytochrome c^{3+}. The inhibition pattern suggests that both the dead-end inhibitor and the nucleotide bind to the same one-electron reduced state of nNOS, E_1. However, 2′AMP exhibited different apparent affinities for the free enzyme in the presence of DCIP and cytochrome c^{3+}, indicating that NADPH and 2′AMP bind to conformationally distinct forms of E_1. The competitive inhibition pattern requires that the binding of NADPH and 2′AMP and the isomerization of E_1 are in rapid equilibrium. If NADPH binding and release were at steady state, 2′AMP would be a noncompetitive inhibitor of NADPH. Thus, the binding of the nucleotide is not the rate-limiting step in the reductive half-reaction.

Another possible rate-limiting step may be the formation of a charge-transfer complex. Biochemical and structural studies have shown that the structurally and functionally related enzymes, FNR and CPR, change conformation to form a charge-transfer complex that positions NADPH close to FAD to facilitate hydride transfer. The crystal structures of rat CPR (*49*) and pea FNR (*8*, *50*) revealed that the aromatic ring of a tryptophan residue in the former and a tyrosine residue in the latter shield the isoalloxazine ring of the FAD from the nicotinamide cofactor. To form the charge-transfer complex, both aromatic side chains reposition themselves so that the nicotinamide ring is at an appropriate distance from the N5 of FAD for hydride transfer. Stopped-flow fluorescence studies have demonstrated that a conserved tryptophan residue in human CPR is mobile and "flips away" from the isoalloxazine ring during the formation of the charge-transfer complex (*51*). Movement of the homologous residue in nNOS, Phe1395, which has been shown by X-ray crystallography to occupy the same position as the tryptophan residue in CPR (*52*), may also be necessary for hydride transfer and may be the origin of the isotopically insensitive rate-limiting step in the reductive half-reaction.

The kinetic mechanisms for the reduction of DCIP and cytochrome c^{3+} were modified to incorporate this step (bold portions of Figures 1 and 2). In both kinetic mechanisms, k_1 and k_2 represent the forward and reverse rate constants for formation of the charge-transfer complex, respectively. Rate equations derived for the kinetic mechanisms in Figures 1 and 2 are consistent with the steady-state initial velocity and inhibition data obtained previously (*24*). With the addition of the charge-transfer complex, $(V/K)_{NADPH}$ is now described by the equation:

$$\frac{V/E_t}{K_A} = \frac{k_1 k_3}{K_{iA}(1 + 1/K)(k_2 + k_3)} \qquad (5)$$

and the expression for $^{D}(V/K)_{NADPH}$ is defined as

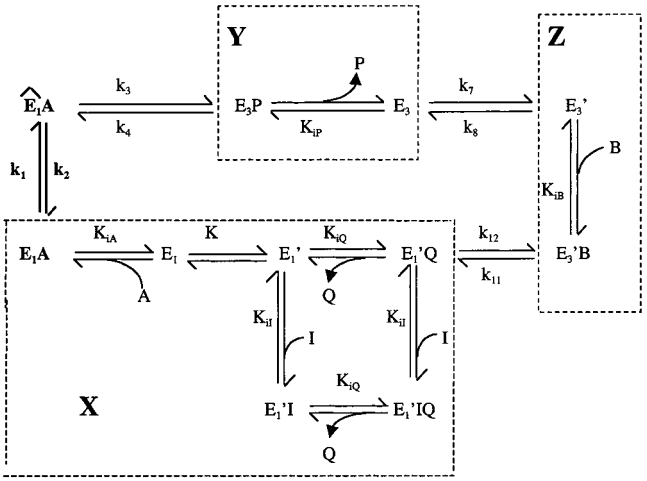

FIGURE 1: Kinetic scheme for a ping-pong bi-bi mechanism for the nNOS-catalyzed reduction of DCIP with a step representing the formation of the charge-transfer complex (E_1A to $\hat{E}_1A$). A, B, P, Q, and I represent NADPH, $DCIP_{ox}$, $NADP^+$, $DCIP_{red}$, and 2′AMP, respectively. The K_i values refer to their respective dissociation constants. E_1 and E_1' are the one-electron (FAD/FMNH•) forms of nNOS that exclusively bind NADPH and 2′AMP, respectively. E_3 and E_3' are the three-electron ($FADH^{\bullet}/FMNH_2$ or $FADH_2/FMNH^{\bullet}$) forms of nNOS that exclusively bind $NADP^+$ and $DCIP_{ox}$, respectively. *K* is the equilibrium constant for the conversion of the two enzyme forms, E_1 and E_1'. The dotted boxes labeled X, Y, and Z indicate the proposed rapid equilibrium segments for the reaction mechanism, where $X = E_1 + E_1' + E_1'I + E_1'IQ + E_1'Q + E_1A$, $Y = E_3P + E_3$, and $Z = E_3' + E_3'B$.

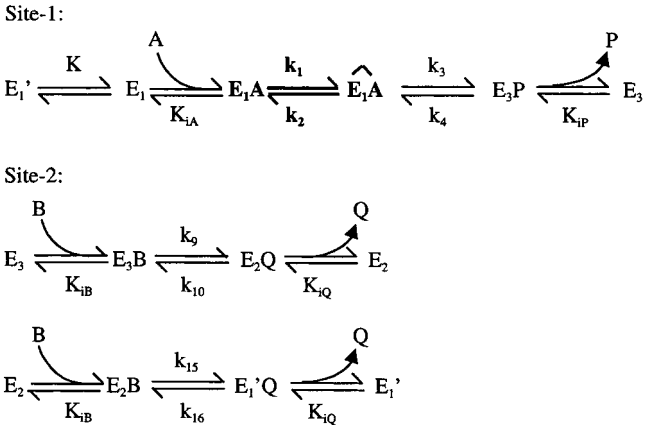

FIGURE 2: Kinetic scheme illustrating the two-site ping-pong mechanism for the nNOS-catalyzed reduction of cytochrome c^{3+} with a step representing the formation of the charge-transfer complex (E_1A to $\hat{E}_1A$). A, B, P, and Q represent NADPH, cytochrome c^{3+}, $NADP^+$, and cytochrome c^{2+}, respectively. E_1 and E_1' are the one-electron (FAD/FMNH•) forms of nNOS that exclusively bind NADPH and 2′AMP, respectively. E_2 and E_3 represent the two- ($FAD/FMNH_2$) and three-electron ($FADH^{\bullet}/FMNH_2$) reduced forms of nNOS. *K* is the equilibrium constant for the conversion of the two enzyme forms, E_1 and E_1'.

$$^{D}(V/K)_{NADPH} = \frac{^{D}k_3 + k_{3H}/k_2}{1 + k_{3H}/k_2} \qquad (6)$$

Equation 6 illustrates that $^{D}(V/K)_{NADPH}$ is a function of k_2, or the rate constant for the reversal of the charge-transfer complex formation. If $k_2 < k_{3H}$, then the value of $^{D}k_3$ is suppressed in $^{D}(V/K)_{NADPH}$. For example, if $^{D}k_3$ is ~7, the classical limit for the intrinsic isotope effect, then for $^{D}(V/K)_{NADPH}$ to range between 1.2 and 1.6, $k_{3H} > k_2$ by 10−30-fold. Alternatively, if $^{D}k_3$ approaches 3, observed if there is

a small change in the C−H and C−D vibrational energy difference between the ground state and the transition state, then k_{3H} need only be 2.5−10-fold greater than k_2. If $k_2 < k_{3H}$, NADPH can be characterized as a "sticky" substrate, as was found for several NADPH dehydrogenases (*34*, *53*, *54*). A substrate is considered sticky if partitioning of the enzyme−substrate complex toward catalysis is favored compared to release from the enzyme (i.e., $k_2 < k_3$; *53*). Vanoni and Mathews proposed that dehydrogenases which exhibit suppression of the isotope effect of hydride transfer in $^{D}(V/K)_{NADPH}$ are optimized for catalytic efficiency of their reductive half-reaction (*34*, *55*). Thus, nNOS would be exhibiting a high forward commitment to catalysis since the E_1−NADPH charge-transfer complex, once formed, would undergo oxidoreduction to form the E_3−$NADP^+$ complex rather than dissociate to form E_1 and NADPH.

The value of the intrinsic deuterium isotope effect can be estimated using the method of Northrop with values obtained for the tritium isotope effects on $(V/K)_{NADPH}$, $^{T}(V/K)_{NADPH}$, and $^{D}(V/K)_{NADPH}$ as long as the deuterium and tritium isotope effects are measured the same way. However, Ryerson et al. demonstrated through transient and steady-state kinetic isotope studies with bacterial NAD(P)H flavoprotein monooxygenases (*56*), which have the same kinetic mechanism for the reductive half-reaction as nNOS, that $^{D}(V/K)_{NADPH}$ and $^{T}(V/K)_{NADPH}$ are composed of different rate constants because they were measured by different experimental methods: optical methods for deuteride transfer and tritium exchange with the solvent from the reduced flavin. The exchange with solvent constitutes the first irreversible step in the reaction sequence. In contrast, the first irreversible step for the reaction with NADPD is the release of $NADP^+$. $^{D}(V/K)_{NADPH}$ and $^{T}(V/K)_{NADPH}$ are not measured by the same method and are composed of different rate constants; therefore, the method of Northrop cannot be used to calculate $^{D}k_3$ for this system.

As described above, $^{D}(V/K)_{NADPH}$ for DCIP and cytochrome c^{3+} reduction are functions of the same rate constants, and as expected, the values for $^{D}(V/K)_{NADPH}$ in the presence of DCIP and cytochrome c^{3+} are similar. The expressions for ^{D}V for the two substrates are different; therefore, they will not necessarily exhibit similar ^{D}V values. As shown in Table 2, the values for ^{D}V for CaM-stimulated reduction of DCIP and cytochrome c^{3+} are not significantly different. However, ^{D}V for basal DCIP reduction is significantly smaller than ^{D}V for basal cytochrome c^{3+} reduction. According to the mechanism illustrated in Figure 1, V for DCIP reduction is defined by the equation:

$$\frac{V}{E_t} = \frac{k_1k_3k_7k_{11}}{k_1k_3k_7 + k_1k_{11}(k_3 + k_7) + k_7k_{11}(k_2 + k_3)} \quad (7)$$

where the rate constants are the same as those in Figure 1. In contrast, V for reduction of cytochrome c^{3+} is a function of the rate constants:

$$\frac{V}{E_t} = \frac{k_1k_3k_9k_{15}}{k_9k_{15}(k_1 + k_2 + k_3) + k_1k_3(k_9 + k_{15})} \quad (8)$$

where k_1, k_2, k_3, k_9, and k_{15} are shown in Figure 2. With k_3 defined as the isotopically sensitive step, ^{D}V equals eq 9 and eq 10 for DCIP and cytochrome c^{3+} reduction, respectively.

$$^{D}V = \frac{^{D}k_3(1 + k_1/k_2) + (k_{3H}/k_2)(x)}{1 + k_1/k_2 + (k_{3H}/k_2)(x)} \quad (9)$$

$$^{D}V = \frac{^{D}k_3(1 + k_1/k_2) + (k_{3H}/k_2)(y)}{1 + k_1/k_2 + (k_{3H}/k_2)(y)} \quad (10)$$

In eq 9, $x = (1 + k_1/k_7 + k_1/k_{11})$, and in eq 10, $y = (1 + k_1/k_9 + k_1/k_{15})$. If k_{3H}/k_2 is ≥10 (assuming the intrinsic isotope effect is near the classical limit and $^{D}(V/K)_{NADPH} \sim 1$; see above), ^{D}V for cytochrome c^{3+} (eq 10) will be smaller than ^{D}V for DCIP (eq 9) only if $y > x$. This suggests that under basal conditions k_7 (the steady-state rate constant for the isomerization of E_3 to E_3') and/or k_{11} (electron transfer from the flavins to DCIP) must be greater than k_9 and/or k_{15} (electron transfer from the flavins to cytochrome c^{3+}).

Comparison of ^{D}V and $^{D}(V/K)$ values in ping-pong mechanisms also provides information concerning the relative rates of the two half-reactions (*57*). For example, a value for ^{D}V similar to $^{D}(V/K)$, as observed for the basal and CaM-stimulated reduction of DCIP, or slightly larger than $^{D}(V/K)$, as seen for cytochrome c^{3+} reduction, suggests that the reductive half-reaction limits the overall reaction rate (*57*). If the reductive half-reaction is more rate limiting, k_1, and/or k_3, < k_7 or k_{11} for DCIP reduction (Figure 1) and k_1, and/or k_3, < k_9 or k_{15} for cytochrome c^{3+} reduction (Figure 2). The analysis of the pH dependence of V, $(V/K)_{NADPH}$, and $(V/K)_{DCIP}$ for basal and CaM-simulated reduction (*59*) suggests that hydride transfer, k_3, is slower than k_7 or k_{11}. Furthermore, noncompetitive inhibition patterns with cytochrome c^{2+} as the inhibitor and NADPH as the variable substrate did not display any curvature for the nNOS- (*24*) and CPR-catalyzed reduction of cytochrome c^{3+} (*58*), indicating that hydride transfer is slower than electron transfer from FMN to cytochrome c^{3+}, k_9 and k_{15}. These results, in conjunction with the SKIE studies discussed below, indicate that the rate of the reductive half-reaction rather than that of the oxidative half-reaction limits the overall reaction rate in both ping-pong kinetic mechanisms.

Stopped-flow experiments with CPR revealed that the formation of the charge-transfer complex occurred rapidly; the apparent rate constant of the first step was >500 s^{-1}, followed by an isomerization of a second transfer complex (∼200 s^{-1}; *51*). The rate of hydride transfer was much slower, ∼3 s^{-1} (*51*). If nNOS were to exhibit the same relative rates for k_1 and k_3, then it follows that the ratio of $k_{3H}/k_2 < k_1/k_2$ since $k_{3H} > k_2$ and $k_1 > k_3$. Equations 9 and 10 illustrate the influence of the k_{3H}/k_2 and k_1/k_2 ratios in the value of ^{D}V for reduction of DCIP and cytochrome c^{3+}, respectively. If $k_1/k_2 > k_{3H}/k_2$ and $k_1 < k_7$ and k_{11} (DCIP reduction) or k_9 and k_{15} (cytochrome c^{3+} reduction), then ^{D}V would be equal for reduction of the two oxidants and equal the value of the intrinsic isotope effect, $^{D}k_3$. However, the value of ^{D}V is lower than the expected value for $^{D}k_3$; therefore, it is suppressed by different amounts by the value of k_{3H}/k_2 multiplied by x and y in eq 9 and eq 10. If $k_1/k_2 < 1$ and $k_1 < k_7$, k_{11}, k_9, and k_{15}, then ^{D}V equals $^{D}(V/K)_{NADPH}$ for the reduction of either DCIP or cytochrome c^{3+}. Since this is clearly not the case for cytochrome c^{3+} reduction, where $^{D}V > ^{D}(V/K)_{NADPH}$, then k_1/k_2 must also contribute substantially to the value of ^{D}V for it to be greater than $^{D}(V/K)_{NADPH}$.

The values for $^{D}(V/K)_{DCIP}$ and $^{D}(V/K)_{cytc}$ were equal to 1 within experimental error. This is consistent with the proposed ping-pong mechanism for these substrates since $^{D}(V/K)_{DCIP}$ and $^{D}(V/K)_{cytc}$ are not functions of k_3 (*24*). The data also suggest that the label exchanges with the solvent prior to reduction of the DCIP or cytochrome c^{3+}. This conclusion is supported by the NADPH stereospecificity study described above as the *pro-R* ^{3}H appeared in the solvent fraction, presumably through solvent exchange while bound to the flavin.

Solvent Kinetic Isotope Effects. Unlike substrate isotope effects which investigate changes in the catalytic rate associated with one isotopic substitution, solvent isotope effects are global in nature as they relate to changes associated with the complete replacement of exchangeable solvent protons with deuterons on the enzyme and substrate (*37*). Deuterium oxide could change the reaction rate by affecting several steps in a multistep mechanism, substrate binding and/or the stability or conformation of the enzyme (*37*). Large SKIE are thought to arise from rate-determining step(s) in which there is direct proton or hydride transfer in the transition state (*37*). The isotope effect would likely be primary, where water is the reactant or functional group(s) on the enzyme or substrate becomes labeled by exchange with the solvent. In contrast, secondary isotope effects, defined by those involving conformational changes in the enzyme caused by the properties of hydrogen bonds, hydrophobic interactions, and other factors, typically yield smaller values for the SKIE.

The large SKIE values of 8 and 30 for $^{D_2O}(V/K)_{cytc}$ observed for the basal and CaM-stimulated reduction of cytochrome c^{3+} suggest that proton uptake directly from the solvent or from an exchangeable site(s) on nNOS or cytochrome c^{3+} is the rate-limiting step in the oxidative half-reaction. The SKIE could arise from a change in the FAD or FMN redox states ($FMNH_2$ to $FMNH^{\bullet}$ and/or $FMNH^{\bullet}$ to FMN) as the substrate is reduced. The magnitude of SKIE may also arise from the effects of D_2O on protein conformation and substrate binding as both nNOS and cytochrome c^{3+} have numerous exchangeable hydrogenic sites, and complex formation between the two proteins requires several hydrogen bond contacts and hydrophobic interactions.

The expression for $(V/K)_{DCIP}$ and $(V/K)_{cytc}$ illustrates further that all of the rate constants and the dissociation constant for the electron acceptor, K_{iB}, are subject to solvent kinetic isotope effects. For DCIP reduction (Figure 1), $(V/E_t)/K_B = k_7k_{11}/K_{iB}(k_7 + k_8)$, and for cytochrome c^{3+} reduction (Figure 2), $(V/E_t)/K_B = k_9k_{15}/K_{iB}(k_9 + k_{15})$. Thus, the large SKIE observed for cytochrome c^{3+} may be attributed to greater increases in K_{iB} and/or decreases in k_9 and/or k_{15} in D_2O compared to H_2O relative to the value of k_7, k_8, k_{11}, and K_{iB} for DCIP. The 4-fold increase in the SKIE on the observed $(V/K)_{cytc}$ may be attributed to a combination of events including further rate limitation of proton transfer, an increase in the number of protons transferred, or the solvent effects on cytochrome c^{3+} binding becoming more pronounced. The level of CaM-stimulated cytochrome c^{3+} reductase activity was approximately 20% greater in D_2O compared to H_2O, indicating that deuterium oxide does not impair the affinity or behavior of the activated cofactor.

The solvent isotope effect on V was approximately 2 for the basal and CaM-stimulated reduction of cytochrome c^{3+}. The relatively small observed ^{D_2O}V suggests that proton transfers causing the large $^{D_2O}(V/K)$ for cytochrome c^{3+} are not rate limiting in the overall steady-state mechanism. These results agree with the primary NADPH(D) substrate isotope effects showing that the reductive half-reaction is more rate limiting. Structural differences in cytochrome c^{3+} induced by D_2O affecting its affinity for nNOS and the value for $^{D}(V/K)_{cytc}$ would not be observed in ^{D}V as it is not a function of substrate binding.

Small SKIE were also observed for $^{D}(V/K)_{NADPH}$ for the basal and CaM-stimulated reduction of cytochrome c^{3+}, indicating that proton transfer is not a rate-limiting step in the reductive half-reaction. The expression for $(V/K)_{NADPH}$ encompasses all of the rate constants from the binding of NADPH up to the first irreversible step. If hydride transfer from C-4 of the nicotinamide ring to N-5 of the flavin constitutes the first irreversible step, the SKIE would not be observed on subsequent proton-transfer steps such as protonation of N-1 of the FAD isoalloxazine ring.

In summary, both primary substrate isotope effects and solvent isotope effects demonstrate that the reductive half-reaction is more rate determining than the subsequent oxidative half-reaction in the ping-pong mechanisms for DCIP and cytochrome c^{3+} reduction, and the presence of Ca^{2+}-CaM does not alter this behavior. The slow step in the reductive half-reaction is not hydride transfer but may be the reversal of the formation of the charge-transfer complex (E_1−NADPH) known to form in CPR and FNR. The slow step in the cytochrome c^{3+} oxidative half-reaction appears to involve the transfer of the proton(s) from the solvent and/or exchangeable sites on nNOS or the substrate.

ACKNOWLEDGMENT

We are grateful to Drs. Sonia Anderson and Dean Malencik for supplying CaM and the CaM−Sepharose column, to Dr. Ted Dawson for giving us the cDNA plasmid construct for rat neuronal NOS, and to Dr. Chris Mathews for T4 bacteriophage dihydrofolate reductase. We also acknowledge the Nucleic Acids and Proteins and Statistics Core Facilities of Oregon State University Environmental Health Sciences Center in conducting these studies.

REFERENCES

1. Marletta, M. A., Hurshman, A. R., and Rusche, K. M. (1998) *Curr. Opin. Chem. Biol. 2*, 656−663.
2. Stuehr, D. J., and Ikeda-Saito, M. (1992) *J. Biol. Chem. 267*, 20547−20550.
3. Bredt, D. S., Hwang, P. M., Glatt, C. E., Lowenstein, C., Reed, R. R., and Snyder, S. H. (1991) *Nature 351*, 714−718.
4. Griffith, O. W., and Stuehr, D. J. (1995) *Annu. Rev. Physiol. 57*, 707−736.
5. Abu-Soud, H. M., and Stuehr, D. J. (1993) *Proc. Natl. Acad. Sci. U.S.A. 90*, 10769−10772.
6. Schimdt, H. H. H. W., Pollock, J. S., Nakane, M., Gorsky, L. D., Forstermann, U., and Murad, F. (1991) *Proc. Natl. Acad. Sci. U.S.A. 88*, 365−369.
7. Cho, H. J., Xie, Q. W., Calaycay, J., Mumford, R. A., Swiderek, K. M., Lee, T. D., and Nathan, C. (1992) *J. Exp. Med. 176*, 599−604.
8. Karplus, P. A., Daniels, M. J., and Herriott, J. R. (1991) *Science 251*, 60−66.
9. Porter, T. D., and Kasper, C. D. (1986) *Biochemistry 25*, 1682−1687.
10. Vermilion, J. L., and Coon, M. L. (1978) *J. Biol. Chem. 253*, 8812−8819.

11. Noble, M. A., Munro, A. W., Rivers, S. L., Robledo, L., Daff, S., Yellowlees, L. J., Shimizu, T., Sagami, I., Guillemette, G., and Chapman, S. K. (1999) *J. Biol. Chem. 38*, 16413−16418.
12. Vermilion, J. L., Balloou, D. P., Massey, V., and Coon, M. J. (1981) *J. Biol. Chem. 256*, 266−277.
13. Gachhui, R., Presta, A., Bentley, D. F., Abu-Soud, H. M., McArthur, R., Brudvig, G., Ghosh, D. K., and Stuehr, D. J. (1996) *J. Biol. Chem. 271*, 20594−20602.
14. Klatt, P., Heinzel, B., John, M., Kastner, M., Bohme, E., and Mayer, B. (1992) *J. Biol. Chem. 267*, 11374−11378.
15. Williams, C. H. J., and Kamin, H. (1962) *J. Biol. Chem. 237*, 587−595.
16. Abu-Soud, H. M., Yoho, L. L., and Stuehr, D. J. (1994) *J. Biol. Chem. 269*, 32047−32050.
17. Sheta, E. A., McMillan, K., and Masters, B. S. (1994) *J. Biol. Chem. 269*, 15147−15153.
18. Roman, L. J., Martasek, P., Miller, R. T., Harris, D. E., de la Garza, M. A., Shea, T. M., Kim, J. J., and Masters, B. S. S. (2000) *J. Biol. Chem. 275*, 29225−29232.
19. Brunner, K., Tortschanoff, A., Hemmens, B., Andrew, P. J., Mayer, B., and Kungl, A. J. (1998) *Biochemistry 37*, 17545−17553.
20. Salerno, J. C., Harris, D. E., Irizarry, K., Patel, B., Morales, A. J., Smith, S. M., Martasek, P., Roman, L. J., Masters, B. S. S., Jones, C. L., Weissman, B. A., Lane, P., Liu, Q., and Gross, S. S. (1997) *J. Biol. Chem. 272*, 29769−29777.
21. Daff, S., Sagami, I., and Shimizu, T. (1999) *J. Biol. Chem. 274*, 30589−30595.
22. Chen, P., and Wu, K. K. (2000) *J. Biol. Chem. 275*, 13155−13163.
23. Roman, L., Miller, T., de la Garaza, M., Kim, J. J. P., and Masters, B. S. S. (2000) *J. Biol. Chem. 275*, 21914−21919.
24. Wolthers, K. R., and Schimerlik, M. I. (2001) *Biochemistry 40*, 4722−4737.
25. Dawson, T. M., and Dawson, V. L. (1996) *Annu. Rev. Med. 47*, 219−227.
26. Muchmore, D. C., McIntosh, L. P., Russell, C. B., Anderson, D. E., and Dahlquist, F. W. (1989) *Methods Enzymol. 177*, 44−73.
27. Moran, R., Sartori, P., and Reich, V. (1984) *Anal. Biochem. 138*, 196−204.
28. Stern, B. K. and Vennesland, B. (1960) *J. Biol. Chem. 235*, 205−210.
29. Pastore, E. J., and Freidkin, M. (1962) *J. Biol. Chem. 237*, 3802−3810.
30. Kornberg, A., and Hornberg, B. L. (1953) in *Biochemical Preparations* (Snell, E. E., Ed.) Vol. 3, p 27, J. Wiley and Sons, New York.
31. Gerber, N. C., and Ortiz de Montellano, P. R. (1995) *J. Biol. Chem. 270*, 17791−17796.
32. Stuehr, D. J., Cho, H. J., Kwon, N. S., Weise, M. F., and Nathan, C. F. (1991) *Proc. Natl. Acad. Sci. U.S.A. 88*, 7773−7777.
33. Peterson, G. (1977) *Anal. Biochem 83*, 346−356.
34. Vanoni, M., and Matthews, R. G. (1984) *Biochemistry 23*, 5272−5279.
35. Gelder, B. F. V., and Slater, E. C. (1962) *Biochim. Biophys. Acta 58*, 593−595.
36. Schowen, K. B., and Schowen, R. L. (1982) *Methods Enzymol. 87*, 551−558.
37. Schowen, R. L. (1977) Solvent isotope effects on enzymatic reactions, *Isotope Effects on Enzyme Catalyzed Reactions* (Cleland, W. W., O'Leary, M. H., and Northrop, D. B., Eds.) pp 64−99, University Park Press, Baltimore, MD.
38. Gruez, A., Pignol, D., Zeghouf, M., Coves, J., Fontecave, M., Ferrer, J. L., and Fontecilla-Camps, J. C. (2000) *J. Mol. Biol. 26*, 199−212.
39. Leclerc, D., Wilson, A., Dumas, R., Gafuik, C., Song, D., Watins, D., Heng, H. H. Q., Rommens, J. M., Scherer, S. W., Rosenblatt, D. S., and Gravel, R. A. (1998) *Proc. Natl. Acad. Sci. U.S.A. 95*, 3059−3064.
40. Massey, V., and Hemmerich, P. (1980) *Biochem. Soc. Trans. 8*, 246−257.
41. Krakow, G., Ammeraal, N., and Vennesland, B. (1965) *J. Biol. Chem. 240*, 1820−1823.
42. Sem, D. S., and Kasper, C. B. (1992) *Biochemistry 31*, 3391−3398.
43. Drysdale, G. R., Spiegle, M. J., and Strittmatter, P. (1961) *J. Biol. Chem. 236*, 2323−2328.
44. Guerrero, M. G., and Vennesland, B. (1975) *FEBS Lett. 51*, 284−286.
45. Larsson, A., and Thelander, L. (1965) *J. Biol. Chem. 240*, 2691−2697.
46. Ammeraal, R. N., Krakow, G., and Vennesland, B. (1965) *J. Biol. Chem. 240*, 1824−1828.
47. Kresge, A. J. (1977) in *Isotope Effects on Enzyme Catalyzed Reactions* (Cleland, W. W., O'Leary, M. H., and Northrop, D. B., Eds.) pp 37−63, University Park Press, Baltimore, MD.
48. Northrop, D. B. (1977) in *Isotope Effects on Enzyme Catalyzed Reactions* (Cleland, W. W., O'Leary, M. H., and Northrop, D. B, Eds.) pp 112−152, University Park Press, Baltimore, MD.
49. Wang, M., Roberts, D. L., Paschke, R., Shea, T. M., Masters, B. S. S., and Kim, J. J. P. (1997) *Proc. Natl. Acad. Sci. U.S.A. 94*, 8411−8416.
50. Deng, Z., Aliverti, A., Zanetti, G., Arakaki, A. K., Ottado, J., Orellano, E. G., Clacaterra, N. B., Ceccarelli, E. A., Carrillo, N., and Karplus, P. A. (1999) *Nat. Struct. Biol. 6*, 847−853.
51. Gutierrez, A., Doehr, O., Paine, M., Wolf, C. R., Scrutton, N. S., and Roberts, G. C. K. (2000) *Biochemistry 39*, 15990−15999.
52. Zhang, J., Martasek, P., Paschke, R., Shea, T., Masters, B. S. S., and Kim, J. J. P. (2001) *J. Biol. Chem. 276*, 37506−37513.
53. Cleland, W. W. (1982) *Methods Enzymol. 87*, 390−405.
54. Podschun, B., Jahnke, K., Schnackerz, K. D., and Cook, P. F. (1993) *J. Biol. Chem. 268*, 3407−3413.
55. Albery, W. J., and Knowles, J. R. (1976) *Biochemistry 15*, 5631−5640.
56. Cummings Ryerson, C., Ballou, D. P., and Walsh, C. (1982) *Biochemistry 21*, 1144−1151.
57. Cook, P. F. (1991) in *Enzyme Mechanisms from Isotope Effects* (Cook, P. F., Ed.) pp 203−230, CRC Press, Boca Raton, FL.
58. Sem, D. S., and Kasper, C. B. (1993) *Biochemistry 32*, 11539−11547.
59. Wolthers, K. R., and Schimerlik, M. I. (2002) *Biochemistry 41*, 205−214.

BI0109461